

Synthesis and Spectral Properties of Phthalimide Based Alkali-clearable Azo Disperse Dyes

Joonseok Koh*, Hoegyong Kim¹, and Jongseung Park²

Department of Textile Engineering, Konkuk University, Seoul 143-701, Korea

¹Personal Care R&D Institute, LG Household & Health Care Ltd., Daejeon 305-342, Korea

²Electronic Chemical Materials Group, Cheil Industries Inc., Gyeonggi-do 437-711, Korea

(Received August 8, 2007; Revised February 27, 2008; Accepted February 29, 2008)

Abstract: The synthesis of a series of phthalimide based azo disperse dyes and their spectral properties were investigated. The azo dyes containing phthalimide and *N*-methyl phthalimide structure in diazo component were synthesized in order to compare their spectral properties. The synthesized dyes developed the color of yellow to violet and the *N*-substitution of the phthalimide gave a bathochromic effect on the color change. Most of the synthesized dyes exhibit negative solvatochromism so that the absorption band of dyes moves toward shorter wavelengths as the polarity of the solvent increases. In the case of halochromic effect, the bathochromic shift decreased steadily with the general electron donating capacity of the substituents in the coupling component, and became negative especially when more powerful electron donating groups are present in the coupling components ring.

Keywords: Phthalimide, Alkali-clearable azo disperse dye, Spectral properties, Molar extinction coefficient, Solvatochromism, Halochromism

Introduction

One of the most troublesome current areas of concern in the textile industry is the pollution brought about by the coloration processes of dyeing and printing. The main problem with the compounds used for applying color is the fact that they are almost always, especially with reference to the original synthetic dyestuffs developed in the 19th or 20th centuries, highly toxic, carcinogenic or both. Until fairly recently, they were released freely into the waste waters from the plant and could be seen boldly proclaiming their presence to all and sundry as a brightly colored, but somewhat nasty, area of water. Of late, however, the industry has been trying valiantly both to reduce the effluent emerging from its dyehouses and to develop less harmful dyes but, although there has been some success in both of these aims, there are still large amounts of dangerous quantities of rejected dyes [1].

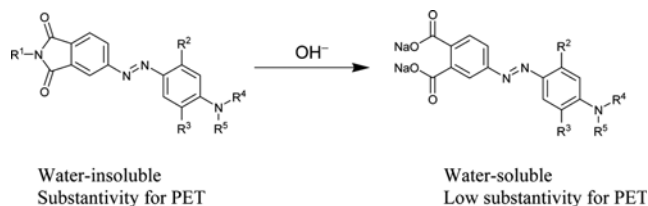
The demand for environmentally friendly dyes of high wet fastness on polyester is increasing. In addition, there are rising global legislative pressures to reduce the impact of dyeing processes on the environment through reductions in effluent discharge as well as in the use of energy and materials. Alkali-clearable disperse dyes offer a means of tackling both of these challenges simultaneously [2-15]. These so-called alkali-clearable disperse dyes obviated the need for sodium hydrosulfite and significantly reduced the cost of effluent treatment.

A previous study [4], which was related to the synthesis of phthalimide based azo disperse dyes and the analysis of alkali-hydrolysis mechanism, found that azo disperse dyes containing phthalimide structure undergo ring opening and

convert to water-soluble product without the breaking of azo bonds under relatively mild alkaline condition (Scheme 1). Therefore, this property can be used advantageously in exhaust dyeing of both 100 % polyester and polyester/cotton blends: phthalimide based azo disperse dyes have an alkali-clearable property which enables alkaline treatment to substitute for reduction clearing and prevent the generation of carcinogenic amines which can be generated in several cases.

The color gamut of phthalimide based 4-(*N,N*-diethylamino) azobenzene dyes which have been synthesized in previous study was orange to red (478-490 nm in DMF) [4]. Recently, we have attempted to synthesize more various disperse dyes which cover the gamut of yellow to violet yellow disperse dyes. Especially, for the yellow shades, hydroxypyridone derivatives were used as coupling components since they provide greenish yellow to orange shades and have significantly high tinctorial strength [16].

In this study, we reported the synthesis of dye intermediates and the subsequent phthalimide based azo disperse dyes and their spectral properties. Specially, the azo dyes containing phthalimide and *N*-methyl phthalimide structure in diazo component were synthesized in order to compare their spectral properties.



Scheme 1. Alkali-hydrolysis of phthalimide based azo disperse dyes.

*Corresponding author: ccdjko@konkuk.ac.kr

Experimental

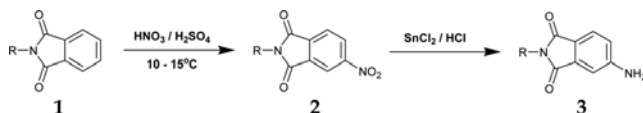
Materials

The chemicals used in the synthesis of disperse dyes were phthalimide, *N*-methylphthalimide, *N,N*-diethylaniline, *N,N*-diethyl-*m*-toluidine, 3-diethylaminoacetanilide, 3-diethylamino-4-methoxyacetanilide, *d*₆-DMSO, *N,N*-dimethylformamide, *p*-dimethylaminobenzaldehyde, H-acid (4-amino-5-hydroxy-2,7-naphthalene disulfonic acid monosodium salt hydrate), sulfuric acid, fuming nitric acid, stannous chloride, sodium nitrite, sodium acetate, ethanol, methanol and cyclohexane. All the chemicals were of laboratory-reagent grade.

Synthesis of Dye Intermediates

The synthesis of 4-aminophthalimide has been described in the previous work [3]. In order to synthesize *N*-methyl-4-aminophthalimide, the procedure was repeated except that in place of non-substituted phthalimide, the *N*-methyl substituted phthalimide were used (Scheme 2).

48 ml of fuming nitric acid (sp.gr.1.50) was added to 280 ml of concentrated sulfuric acid (sp.gr.1.84) in 1-liter beaker and *N*-methylphthalimide (**1**) (0.272 mol) was stirred in as rapidly as possible while the temperature of the nitrating mixture was kept between 10 °C and 15 °C. The



Scheme 2. Overall schemes of diazo component synthesis (R=H, CH₃).

reaction mixture was allowed to warm slowly to room temperature. After 16 hours, the precipitated crude nitrated product (**2**) was isolated, washed four times with ice water, and purified by crystallization from ethanol, giving buff-colored plate (Scheme 2) [17].

A solution of stannous chloride (184 g) in 300 ml of hydrochloric acid (sp.gr.1.14) and 48 ml of water was prepared. The solution was heated up to the temperature of 85 °C and *N*-methyl-4-nitrophthalimide (**2**) (50 g) was added and stirred. After 90 min, the precipitate was collected at 0 °C and washed with hot water until free from acid, the hydrochloride thus being completely hydrolyzed and the base was obtained as golden-yellow needles. This aminated product (**3**) was purified by crystallization from acetic acid, giving golden-yellow needles (Scheme 2) [18].

The structures and yield of synthesized dye intermediates in present study are given in Table 1.

The coupling component, 1,4-dimethyl-2-hydroxy-5-cyano-6-pyridone (**4**) was prepared using previously described procedures (Scheme 3) [13,19-21] and the other coupling components, *o*- and/or *m*-substituted *N,N*-diethylaniline (**5-8**) were purchased from Sigma Aldrich (Table 2).

Synthesis of Dyes

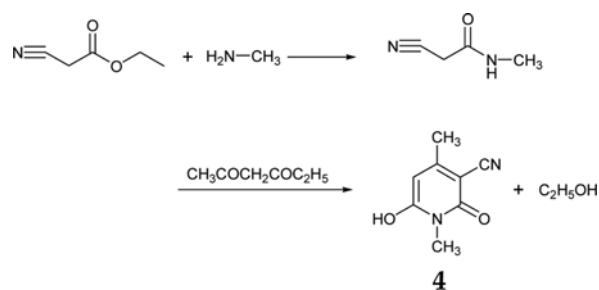
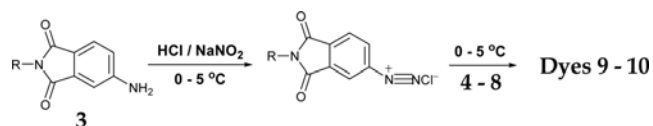
0.025 mol of 4-aminophthalimide (**3**, R=H) was diazotized in 8.6 ml of 35 % HCl and 90 ml of water, by adding 0.025 mol of NaNO₂ at a temperature of 0~5 °C. After 5~6 hours, the completion of diazotization was checked by *p*-dimethylaminobenzaldehyde solution and the pH value of the diazotized solution was adjusted to the range 5~6 by adding sodium acetate. Then, the solution of diazonium salt was filtered and

Table 1. The structures and yields of the synthesized dye intermediates **2** and **3**

Intermediate	Name	Structure	Appearance	Crude yield (%)	Pure yield (%)
2a	4-nitrophthalimide		Creamy powder	78.5	63.4
2b	<i>N</i> -methyl-4-nitrophthalimide		Creamy powder	86.0	77.7
3a	4-aminophthalimide		Yellow powder	49.0	40.3
3b	<i>N</i> -methyl-4-aminophthalimide		Lemon powder	68.6	60.2

Table 2. Coupling components used in the present study

Coupling components	Structure	Name
4		1,4-dimethyl-2-hydroxy-5-cyano-6-pyridone
5		<i>N,N</i> -diethylaniline
6		<i>N,N</i> -diethyl-m-toluidine
7		3-diethylaminoacetanilide
8		3-diethylamino-4-methoxyacetanilide

**Scheme 3.** Overall schemes of coupling components synthesis.**Scheme 4.** Synthesis of phthalimide based azo disperse dyes (9 : R=H, 10 : R=CH₃).

added to a solution containing 0.025 mol of coupling component (4-8), 50 ml of water, and 4.3 ml of 35 % HCl. After 5~6 hours, the completion of coupling was checked by 10 % H-acid solution, and the precipitated dye (9) was filtered, washed with water, and dried. The dyes were purified by crystallization from acetone (9a) or methanol or

Table 3. The structures and yields of the synthesized dyes 9 and 10 in the present study

Chemical structures	Dye	R ¹	R ²	R ³	Crude yield (%)	Pure yield (%)
	9a	H	—	—	80.5	53.5
	9b	H	H	H	79.2	44.0
	9c	H	CH ₃	H	91.4	64.1
	9d	H	NHOCH ₃	H	83.0	45.3
	9e	H	NHOCH ₃	OCH ₃	72.8	43.2
	10a	CH ₃	—	—	87.0	72.8
	10b	CH ₃	H	H	77.2	49.1
	10c	CH ₃	CH ₃	H	81.0	62.4
	10d	CH ₃	NHOCH ₃	H	83.1	68.6
	10e	CH ₃	NHOCH ₃	OCH ₃	68.8	63.1

acetone (**9b-9e**) and washing with cyclohexane except dye **9a**. Also, in order to synthesize *N*-methylphthalimide based azo disperse dyes (**10**), the same procedure was repeated except that in place of phthalimide, the *N*-methylphthalimide was used as the diazo component (Scheme 4) [4]. The structures and yield of dyes synthesized in the present study are given in Table 3.

Characterization

The ¹H-NMR spectra were obtained with a JNM-FX 200 (JEOL, 200 MHz) for solutions in an appropriate deuterated solvent. Elemental analyses were carried out on a CHNS-932 (LECO) for C, H, N and S. The IR spectra were obtained with a FT-IR Spectrophotometer (Perkin Elmer Spectrum 2000, 16 scans).

Melting points were determined using a DSC 7 (Perkin-Elmer, heating rate 5 °C/min, N₂ gas). The absorption spectra were measured in 1 cm quartz cells on a UV-Visible spectrophotometer (HP8452A, Hewlett Packard).

The spectral properties were measured in quartz cells on UV-Visible spectrophotometer. Dye (10-14 mg) was dissolved in DMF, transferred to a volumetric flask (100 ml) and the solution was made up to the mark. An aliquot was diluted appropriately (5 ml to 100 ml or 10 ml to 100 ml) so that the resulting solution had an absorbance in the range 0.6-1.5. The procedure was performed three times for each dye, λ_{max} and ε_{max} and three values were averaged to four significant figures, respectively. Molar extinction coefficient value (ε_{max}) was calculated as follows;

$$A = \epsilon c l \quad (1)$$

where, *A*=absorbance

ε=molar extinction coefficient (l mol⁻¹cm⁻¹)

c=the concentration of solute (mol/l)

l=path length through the sample (cm)

When the width of cell, namely, path length through the sample is 1 cm and absorbance was observed at λ_{max}, the molar extinction coefficient (ε_{max}) was obtained from the following equation.

$$\epsilon_{\max} = A c^{-1} l^{-1} \text{ (l mol}^{-1} \text{ cm}^{-1}\text{)} \quad (2)$$

The width of the absorption band at half the peak height (Δν_{1/2}) was also recorded. In addition, values of λ_{max} of each dye in chloroform and in ethanol were also obtained, where possible.

Spectra of dyes in acidic solution were recorded, the solutions being prepared by the addition of conc. HCl solution to a solution of the dye in ethanol (EtOH:conc. HCl=2:1 by volume).

Results and Discussion

Characterization of Dye Intermediates and Dyes

The NMR, elemental analysis and mass spectroscopy data are shown in Tables 4-6.

The nitrophthalimides (**3a** and **3b**) showed higher melting points compared with non-aminophthalimide (**2a** and **2b**) probably due to their higher polarity. However, *N*-methyl-

Table 4. ¹H-NMR data of the synthesized dye intermediates (**2** and **3**) and dyes(**9** and **10**)

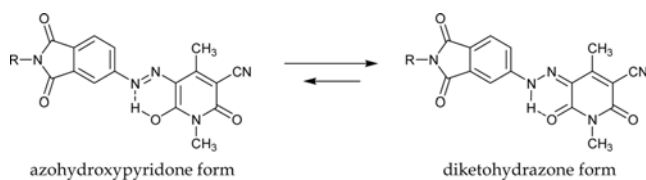
Intermediates/dyes	Chemical shift (DMSO- <i>d</i> ₆ , Δ)
2a	8.0(1H, d, Ar H), 8.4(1H, d, Ar H), 8.6(1H, q, Ar H), 11.8(1H, s, imide N-H)
2b	3.0(3H, s, imide N-CH ₃), 8.1(1H, d, Ar H), 8.4(1H, d, Ar H), 8.6(1H, q, Ar H)
3a	6.3(2H, s, Ar-NH ₂), 6.79(1H, q, Ar H), 6.86(1H, d, Ar-H), 7.4(1H, d, Ar-H), 10.7(1H, s, imide N-H)
3b	2.9(3H, s, imide N-CH ₃), 6.4(2H, s, Ar NH ₂), 6.7(1H, q, Ar-H), 6.9(1H, d, Ar-H), 7.4(1H, d, Ar-H)
9a	2.5(3H, s, Ar-CH ₃), 3.3(3H, s, ArN-CH ₃), 7.8(2H, d, Ar-H), 8.0(1H, q, Ar-H), 11.4(imide N-H)
9b	1.1(6H, t, Ar-N-C-CH ₃), 3.5(4H, q, Ar-NH ₂ -C), 6.8(2H, d, Ar-H), 7.8(1H, d, Ar-H), 7.9(1H, d, Ar-H), 8.0(1H, d, Ar-H), 8.1(1H, q, Ar-H), 11.4(1H, s, imide N-H)
9c	1.1(6H, t, Ar-N-C-CH ₃), 2.6(3H, s, Ar-CH ₃), 3.4(4H, q, Ar-NCH ₂ -C), 6.6(2H, t, Ar-H), 11.4(1H, s, imide N-H)
9d	1.1(6H, t, Ar-N-C-CH ₃), 2.5(3H, s, Ar-NHCO-CH ₃), 3.4(4H, q, Ar-NCH ₂ -C), 6.6(1H, q, Ar-H), 7.7(1H, d, Ar-H), 7.8(1H, d, Ar-H), 7.9(1H, d, Ar-H), 8.2(1H, q, Ar-H), 10.6(1H, s, Ar-NH-CO-), 11.4(1H, s, imide N-H)
9e	1.1(6H, t, Ar-N-C-CH ₃), 2.2(3H, s, Ar-NHCO-CH ₃), 3.7(4H, q, Ar-NCH ₂ -C), 3.8(3H, s, Ar-OCH ₃), 7.1(1H, s, Ar-H), 7.8(1H, s, Ar-H), 7.9(1H, d, Ar-H), 8.2(2H, d, Ar-H), 10.1(1H, s, Ar-NH-CO), 11.4(1H, s, imide N-H)
10a	2.5(3H, s, Ar-CH ₃), 3.0(3H, s, imide N-CH ₃), 3.25(3H, s, ArN-CH ₃), 7.9(1H, Ar-H), 8.1(2H, Ar-H)
10b	1.1(6H, t, Ar-N-C-CH ₃), 3.0(3H, s, imide N-CH ₃), 3.5(4H, q, Ar-NCH ₂ -C), 6.8(2H, d, Ar-H), 7.8(1H, d, Ar-H), 7.9(1H, d, Ar-H), 8.0(1H, d, Ar-H), 8.1(1H, q, Ar-H)
10c	1.1(6H, tr-N-C-CH ₃), 2.6(3H, s, Ar-CH ₃), 3.0(3H, s, imide N-CH ₃), 3.5(4H, q, r-NCH ₂ -C), 6.9(2H, t, Ar-H), 7.7(1H, t, Ar-H), 7.9(1H, d, Ar-H), 8.0(1H, d, Ar-H), 8.1(1H, q, Ar-H)
10d	1.1(6H, t, Ar-N-C-CH ₃), 2.2(3H, d, Ar-NHCO-CH ₃), 3.0(3H, s, imide N-CH ₃), 3.4(4H, q, Ar-NCH ₂ -C), 6.6(1H, q, Ar-H), 7.7(1H, d, Ar-H), 7.8(1H, d, Ar-H), 7.9(1H, d, Ar-H), 8.1(1H, d, Ar-H), 8.2(1H, q, Ar-H), 10.6(1H, s, Ar-NH-CO-)
10e	1.1(6H, t, Ar-N-C-CH ₃), 2.2(3H, d, Ar-NHCO-CH ₃), 3.0(3H, s, imide N-CH ₃), 3.4(4H, q, Ar-NCH ₂ -C), 3.8(3H, s, Ar-OCH ₃), 7.3(q, H, s, Ar-H), 7.8(1H, s, Ar-H), 7.9(1H, D, Ar-H), 8.2(1H, d, Ar-H), 8.3(1H, d, Ar-H), 10.1(1H, s, Ar-NH-CO-)

Table 5. Elemental analysis data of the synthesized dye intermediates (**2** and **3**) and dyes (**9** and **10**)

Structures	Calc./Obs. (%)	C	H	N	
Dye intermediates	2a	Calc. (%)	50.01	2.10	14.58
		Obs. (%)	49.63	2.10	14.04
	2b	Calc. (%)	52.43	2.93	13.59
		Obs. (%)	52.05	2.89	13.51
	3a	Calc. (%)	59.26	3.73	17.28
		Obs. (%)	59.11	3.70	17.36
3b	Calc. (%)	61.36	4.58	15.90	
	Obs. (%)	61.51	4.59	15.94	
Dyes	9a	Calc. (%)	56.98	3.29	20.76
		Obs. (%)	55.87	3.45	19.89
	9b	Calc. (%)	67.07	5.63	17.38
		Obs. (%)	67.03	5.64	17.55
	9c	Calc. (%)	67.84	5.99	16.66
		Obs. (%)	67.81	6.00	16.55
	9d	Calc. (%)	63.31	5.58	18.46
		Obs. (%)	63.04	5.60	17.10
	9e	Calc. (%)	61.60	5.66	17.10
		Obs. (%)	60.49	5.65	17.08
	10a	Calc. (%)	58.12	3.73	19.93
		Obs. (%)	58.18	3.73	19.93
	10b	Calc. (%)	67.84	5.99	16.66
		Obs. (%)	67.51	5.94	16.59
	10c	Calc. (%)	68.55	6.33	15.99
		Obs. (%)	68.37	6.31	15.98
	10d	Calc. (%)	64.11	5.89	17.80
		Obs. (%)	63.94	5.81	17.74
	10e	Calc. (%)	62.40	5.95	16.54
		Obs. (%)	62.41	5.96	16.51

Table 6. Melting point and mass analysis of the synthesized dye intermediates (**2** and **3**) and dyes (**9** and **10**)

Chemicals	No.	Mol. weight	Mass (M ⁺)	m.p. (°C)
Intermediates	2a	192.13	192	201
	2b	206.16	206	178
	3a	162.04	162	291
	3b	176.17	176	247
Dyes	9a	337.29	338	330
	9b	322.36	323	258
	9c	336.39	337	252
	9d	379.41	380	266
	9e	409.44	409	228
	10a	351.32	352	324
	10b	336.39	337	188
	10c	350.41	351	205
	10d	393.44	393	200
	10e	423.41	423	174

**Scheme 5.** Equilibrium of the arylazopyridone dye containing a phthalimide moiety.

phthalimides (**2b** and **3b**) showed lower melting points compared with the non-substituted phthalimides (**2a** and **3a**) probably due to the lower chain packing efficiency. Also, the similar trends were observed in the synthesized phthalimide based dyes.

Especially, in the case of azohydroxypyridone dyes (**9a** and **10a**), it is well known that the hydrazone form of hydroxypyridone dye is predominant over the azo form in the solid state and acidic solutions (Scheme 5) [22]. The FT-IR spectra of the dyes provide some characteristic results to prove this. The IR spectra showed two carbonyl peak at 1715 and 1630 cm^{-1} for the hydrogen-bonded one and free one while the intermediates (**4**) show only one vibrational peak at 1621-1665 cm^{-1} , which is consistent with the previous results [13,22-24].

The mass analysis results together with melting points of synthesized dyes are shown in Table 6. The mass analysis results are consistent with the theoretical molecular weight and this data supports that the dyes are synthesized properly. In the case of melting points, although it would be unwise to attempt to explain in detail their relative values, because of the complex dependence of the melting points on a number of factors, a few general trends can be accounted for. The dyes prepared from a low melting diazo component (*N*-methyl-4-aminophthalimide, m.p. 247 °C) tended to have low melting points themselves and the factors determining high melting points were preserved in the dyes from a high melting diazo component (4-aminophthalimide, m.p. 291 °C): dyes **10** containing a phthalimide moiety showed lower melting points than dyes **9** containing a *N*-methylphthalimide. The lower melting points of dyes **9** could be attributed to the low chain packing efficiency of dye molecules due to the steric hindrance of *N*-methyl group as mentioned earlier.

Especially, the azohydroxypyridone dyes (**9a** and **10a**) showed much higher melting compared with 4-aminoazobenzene dyes (**9b-9e** and **10b-10e**) probably due to the higher polarity of pyridone structure. Generally, it is presumed that, the dyes which contain more polar groups tend to have higher melting points.

Absorption Spectra

The synthesized dyes developed the color of yellow having λ_{max} 444 nm, to violet having λ_{max} 528 nm in DMF. Details of the visible absorption spectra (λ_{max} , ϵ_{max} and $\Delta V_{1/2}$) of phthalimide based dyes are summarized in Tables 7-9.

It is well known that λ_{\max} values are directly proportional to the electronic power of the substituents in the benzenoid system [25]. Since the electronic transition in these compounds involves a general migration of electron density from the

Table 7. Spectral properties of the synthesized dyes **9** and **10**

Dye	λ_{\max} (DMF) (nm)	ϵ_{\max} (DMF) ($l\ mol^{-1}\ cm^{-1}$)	$\Delta\nu_{1/2}$ (DMF) (cm^{-1})	f^a (DMF)
9a	444	29800	5296	0.682
9b	484	33800	4403	0.643
9c	498	34400	4365	0.649
9d	504	41500	3814	0.684
9e	526	30800	4169	0.555
10a	452	29100	5465	0.687
10b	490	34500	4295	0.640
10c	498	36100	4365	0.681
10d	508	41500	3793	0.680
10e	528	32600	3989	0.562

^a f , Oscillator strength (f)= $4.32 \times 10^{-9} \times \Delta\nu_{1/2} \times \epsilon_{\max}$

Table 8. Solvatochromic effects of the synthesized dyes **9** and **10**

	λ_{\max} (CHCl ₃) (nm)	$\Delta\lambda^a$ (nm)	λ_{\max} (EtOH) (nm)	$\Delta\lambda^b$ (nm)	λ_{\max} (DMF) (nm)
9a	430	2	432	14	444
9b	486	-10	476	-2	484
9c	500	-16	484	-2	498
9d	512	-14	498	-8	504
9e	544	-24	520	-18	526
10a	434	-2	432	18	452
10b	484	-4	480	6	490
10c	498	-10	488	0	498
10d	510	-8	502	-2	508
10e	540	-14	526	-12	528

$\Delta\lambda^a = \lambda_{\max}(\text{EtOH}) - \lambda_{\max}(\text{CHCl}_3)$, $\Delta\lambda^b = \lambda_{\max}(\text{DMF}) - \lambda_{\max}(\text{CHCl}_3)$ in nm.

Table 9. Halochromic effects of the synthesized dyes **9** and **10**

	λ_{\max} (EtOH) (nm)	λ_{\max} (HCl/EtOH) (nm)	$\Delta\lambda^a$ (nm)
9a	432	432	0
9b	476	512	36
9c	484	506	22
9d	498	486	-12
9e	520	462	-58
10a	432	436	4
10b	480	512	32
10c	488	510	22
10d	502	486	-16
10e	526	462	-64

$\Delta\lambda^a = \lambda_{\max}(\text{HCl/EtOH}) - \lambda_{\max}(\text{EtOH})$ in nm.

donor group towards the azo group, the greatest effect in terms of longer wavelength is achieved by placing the substituents in the positions *ortho*- or *para*- to azo group, for effective conjugation [26,27].

The phthalimide based azo disperse dyes absorb maximally at 5 to 14 nm shorter wavelengths in ethanol compared to the visible absorption spectra of the 4-(*N,N*-diethylamino)-4'-nitroazobenzene dyes containing the same coupling components. This result indicates that the electron withdrawing property of phthalimide moiety is less powerful than the typical diazo component, 4-nitroanilines.

The absorption wavelength can also be increased by increasing the number of electron donor groups in the coupling component and the most favorable positions are 2- and 5- relative to the azo group. Thus, the more effective the donor substituent, the more bathochromic is the shift, as shown in Table 7; of the synthesized phthalimide based azo dyes, the dyes **9e** and **10e** containing 2-acylamino-5-methoxy substituent showed greater bathochromic shift than the rest of them. Couplers that possess a 2-acylamino group are commonly encountered in commercial dyes, often in conjunction with a 5-methoxy group. The groups exert a synergistic bathochromic shift, although any intensity increase caused by the amide function is counterbalanced by sterically-induced hypsochromism owing to the methoxy group hindering the terminal group.

Half-band widths of the absorption bands in DMF were determined (Table 7). In addition to the effect on λ_{\max} , substituents also cause a change in the half-band width values ($\Delta\nu_{1/2}$). The value of $\Delta\nu_{1/2}$ is a convenient criterion for the evaluation of the hue brightness of dyes; dyes with low values of $\Delta\nu_{1/2}$ show bright hues while those with high values of $\Delta\nu_{1/2}$ show dull hues. Dyes **9d** and **10d** which contain acylamino group at *ortho*- position showed the narrowest half-band width, probably because the tendency of the resonance stabilization increases as the number of potential hydrogen-bonding groups increases. However, there were no remarkable differences between the non-substituted phthalimide based azo dyes (**9a-9e**) and the *N*-methyl substituted analogues (**10a-10e**).

In the case of tinctorial strength, it is well known as a 'rule of thumb' that molar extinction coefficient increases as λ_{\max} increases. For the series of synthesized dyes, ϵ_{\max} values tend to increase with increasing electron donating capacity in the coupling component ring except dyes **9e** and **10e**. The low extinction coefficients of dyes **9e** and **10e** is probably due to the steric hindrance between methoxy group and *N,N*-diethyl group. According to the PPP MO model, the oscillator strength (f) rather than the molar extinction coefficient (ϵ_{\max}) gives true measure of tinctorial strength since it expresses the area under the absorption curve (equation 3).

$$f = 4.32 \times 10^{-9} \times \Delta\nu_{1/2} \times \epsilon_{\max} \quad (3)$$

where $\Delta\nu_{1/2}$ is the half-band width, i.e. the width of the

absorption band, in cm^{-1} , at $\epsilon = 1/2 \epsilon_{\text{max}}$.

Thus, the dye with a high ϵ_{max} value but narrow absorption curve (i.e. low $\Delta\nu_{1/2}$) could be tinctorially weaker than the dye which, although it has a lower ϵ_{max} value, has broader absorption curve. i.e. although **9a** and **10a** have lowest ϵ_{max} , they are tinctorially stronger than the other dyes which has narrower absorption curve.

Solvatochromic Effects

Generally, in many dye molecules, the ground state is less polar than the excited state so that a polar solvent will tend to stabilize the excited state more than the ground state, leading to a bathochromic shift in the absorption maximum, which is termed 'positive solvatochromism' ($\Delta E_2 < \Delta E_1$, Figure 1). The interaction of a solvent with a dye molecule is greater in polar solvents, for example ethanol, which possess a strong permanent dipole, and is most pronounced with a solute molecule that contains a permanent dipole. As the difference between the polarity of the ground and excited states is increased by the successive introduction of stronger electron-donating groups in the coupling component of an azo dye, more marked positive solvatochromism is observed [26].

However, it is clear from Table 8 that most of the synthesized dyes exhibit negative solvatochromism so that the absorption band of dyes moves toward shorter wavelengths as the polarity of the solvent increases. The negative solvatochromic shift strongly indicates the existence of intermolecular hydrogen bonding between the dye molecules in the ground state and the solvent. Thus, the resultant stabilization of the ground state by the H-bonding contribution could account for the hypsochromic shifts between chloroform and more polar solvent since ΔE for the transition is increased ($\Delta E_3 > \Delta E_1$, Figure 1). Especially, only in the case of arylazopyridone dyes (**9a** and **10a**), slight positive solvatochromic shift was

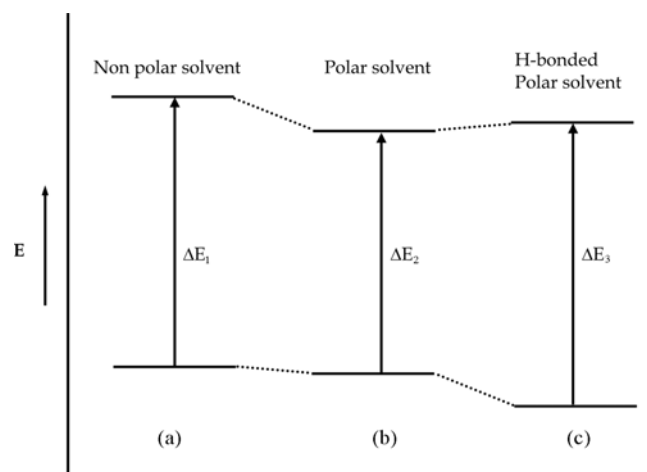


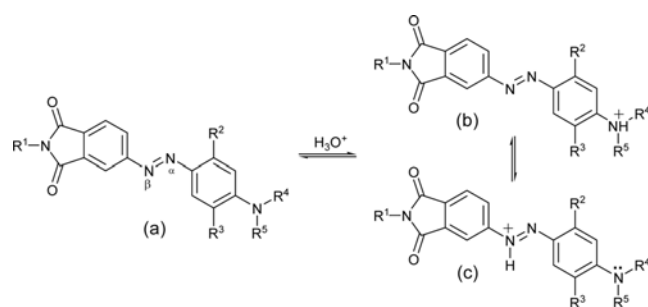
Figure 1. Energy diagram associated with solvatochromism. (a) situation in non-polar solvents (b) situation in polar solvents (c) situation in polar solvent which forms intramolecular hydrogen bonding with dyes.

observed between chloroform and more polar solvents.

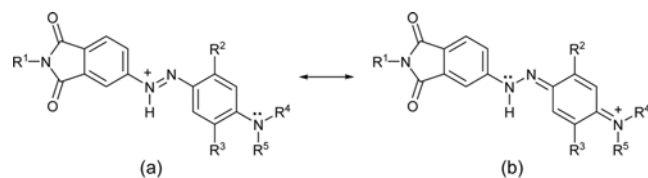
Halochromic Effects

Many dyes derived from 4-aminoazobenzene undergo a pronounced change in color in the presence of acids [26]. This change in the color of a chromogen on addition of acid is referred to as 'halochromism'. Although many types of azo dye show this effect, for example, those containing benzene, naphthalene and heterocyclic rings, it only occurs when the amino group is *para* to the azo linkage.

Protonation of a phthalimide based azo dyes can occur either at the terminal amino group to give ammonium tautomer (b), or at the β -nitrogen atom of the azo group to give the azonium tautomer (c) (Scheme 6). The ammonium tautomer, in which the amino group no longer possesses a free lone pair of electrons, resembles azobenzene substituted in the *para* position with an electron-withdrawing group and thus absorbs in the ultra-violet region with a lower ϵ_{max} than the neutral dye. Because the ammonium tautomers normally absorb at much shorter wavelength, owing to the interruption of electron donation by protonation, little attention has been paid to their investigation. In contrast, the azonium tautomers provide a red-shifted absorption band and more intense colors than the parent dyes, and consequently are of greater interest. The azonium tautomer contains a delocalized positive charge (Scheme 7) and hence bears some resemblance to cyanine dyes. Applying resonance theory to the azonium cation, the ground state of the molecule is best represented by (b) and excited state by (a) in Scheme 7. Since both the ground state and the first excited state are positively charged, no energetically unfavorable charge separation occurs on excitation from the ground state to the first excited state –



Scheme 6. Protonation equilibria of phthalimide based azo dyes ; (a) neutral dye, (b) ammonium tautomer, and (c) azonium tautomer.



Scheme 7. Delocalization of positive charge in the azonium tautomer (a \leftrightarrow b).

only a redistribution of charge. Consequently, the energy separation between the two states is less for the azonium tautomer than that for the neutral dye. It follows that the ground and first excited state are structurally more similar than in the case of neutral azo dyes, which leads to more bathochromic shift (usually bluish-red), more tinctorial strength and narrower absorption band and hence brighter dyes than the neutral dye [16].

In general, bathochromic shifts combined with increased color intensity are often observed for the azonium ion. The shift is termed 'positive halochromism', whereas the opposite phenomenon is defined as 'negative halochromism' [28,29]. Comparison with the neutral dye, in the azonium species, the ground and excited states are much closer together in energy terms so that a bathochromic shift of the first absorption band is observed on protonation (positive halochromism).

Examples of negative halochromism are quite rare when only one electron-withdrawing group is present unless the dye has the electron donating group in coupling component ring. A very powerful electron-withdrawing group or a combination of strong electron acceptors is needed. Alternatively, relatively simple heterocyclic diazo or coupler residues are sufficient to cause negative halochromism.

From Table 9, it can be seen that the bathochromic shift decreased steadily with the general electron donating capacity of the substituents in coupling components ring, and in fact became negative especially when more powerful electron donating groups are present in the coupling components ring. Dyes **9d**, **9e**, **10d** and **10e** containing powerful electron donating groups in coupling component ring show negative halochromism due to the strong electronic effect while dyes **9a-9c** and **10a-10c** containing just not more than one electron donating group in coupling components showed positive halochromism. The experimental results show that the substituents R², R³ affects the halochromism to an extent which depends on their electron donating power. Therefore, by using appropriate substituents, it is possible to design dyes that show no color change in acid ($\Delta\lambda=0$) and which in theory should make good textile dyes, where pH sensitivity is undesirable [30]. Of the synthesized phthalimide based dyes, arylazopyridone dyes (**9a** and **10a**) exhibited negligibly small color change under acidic condition, probably because of the stabilization by hydrogen bonding.

Conclusion

A series of phthalimide based azo disperse dyes were prepared from the coupling reaction between 4-amino-phthalimides and several coupling components (i.e. o- and/ or m- substituted *N,N*-diethylanilines and hydroxypyridone) and their thermal properties and spectral properties were investigated.

The dyes containing a phthalimide moiety showed lower melting points than the dyes containing a *N*-methylphthalimide.

The lower melting points of the former dyes could be attributed to the low chain packing efficiency of dye molecules due to the steric hindrance of *N*-methyl group. Especially, the azohydroxypyridone dyes showed much higher thermal stability compared with 4-aminoazobenzene dyes probably due to the higher polarity of pyridone structure.

The synthesized dyes developed the color of yellow having λ_{\max} 444 nm, to violet having λ_{\max} 528 nm in DMF and the *N*-substitution of the phthalimide gave a bathochromic effect on the color change. The dyes which contain acylamino group at ortho- position showed the narrowest half-band width, probably because the tendency to the resonance stabilization increases as the number of potential hydrogen-bonding groups increases. However, there were no remarkable differences between the non-substituted phthalimide based azo dyes and the *N*-methyl substituted analogues. In the case of tinctorial strength, for the series of synthesized dyes, ϵ_{\max} values tend to increase with increasing electron donating capacity in the coupling component ring.

Most of the synthesized dyes exhibit negative solvatochromism so that the absorption band of dyes moves toward shorter wavelengths as the polarity of the solvent increases. The negative solvatochromic shift strongly indicates the existence of intermolecular hydrogen bonding between the dye molecules and the solvent. Especially, only in the case of arylazopyridone dyes, slight positive solvatochromic shift was observed between chloroform and more polar solvents.

In the case of halochromic effect, the bathochromic shift decreased steadily with the general electron donating capacity of the substituents in coupling components ring, and in fact became negative especially when more powerful electron donating groups are present in the coupling components ring. Of the synthesized phthalimide based dyes, arylazopyridone dyes exhibited negligibly small color change under acidic condition, probably because of the stabilization by hydrogen bonding.

Acknowledgements

This paper was supported by Konkuk University in 2008.

References

1. K. Slater, "Environmental Impact of Textiles - Production, Processes and Protection", p.81, Woodhead Publishing Ltd., Cambridge, 2003.
2. B. R. Fishwick, V. Boyd, and B. Glover, *US Patent* 1,456,58 (1976).
3. J. S. Koh and J. P. Kim, *Dyes Pigm.*, **37**, 265 (1998).
4. J. S. Koh and J. P. Kim, *J. Soc. Dyers. Colour.*, **114**, 121 (1998).
5. J. Koh and A. J. Greaves, *Dyes Pigm.*, **50**, 117 (2001).
6. J. Koh, *Ph. D. Thesis*, Seoul National University, 2002.
7. J. Koh, J. D. Kim, and J. P. Kim, *Dyes Pigm.*, **56**, 17

- (2003).
8. J. Koh, A. J. Greaves, and J. P. Kim, *Dyes Pigm.*, **56**, 60 (2003).
 9. J. Koh, A. J. Greaves, and J. P. Kim, *Dyes Pigm.*, **60**, 155 (2004).
 10. J. Koh and J. P. Kim, *Coloration Technology*, **120**, 56 (2004).
 11. J. Koh and J. P. Kim, *Fibers and Polymers*, **5**, 134 (2004).
 12. J. Koh, H. Y. Yoo, and J. P. Kim, *Coloration Technology*, **120**, 156 (2004).
 13. J. Koh, S. Kim, and J. P. Kim, *Coloration Technology*, **120**, 241 (2004).
 14. J. Koh, *Dyes Pigm.*, **64**, 17 (2005).
 15. J. Koh, *Dyes Pigm.*, **69**, 233 (2006).
 16. P. F. Gordon and P. Gregory, "Organic Chemistry in Colour", p.108, Springer-Verlag, London, 1982.
 17. E. H. Huntress and R. L. Shriner, "Organic Syntheses", Collective Vol. 2, p.459, Wiley & Sons, New York, 1943.
 18. H. Karatani, *Bull. Chem. Soc. Jpn.*, **60**, 2023 (1987).
 19. C. C. Chen and I. J. Wang, *Dyes Pigm.*, **15**, 69 (1991).
 20. K. A. Bello, *Dyes Pigm.*, **28**, 83 (1995).
 21. J. J. Lee, N. K. Han, W. L. Lee, J. H. Choi, and J. P. Kim, *Coloration Technology*, **118**, 154 (2002).
 22. N. Ertan and P. Gurkan, *Dyes Pigm.*, **33**, 137 (1997).
 23. A. Lycka and V. Machacek, *Dyes Pigm.*, **7**, 171 (1986).
 24. Q. Peng, M. Li, K. Gao, and L. Cheng, *Dyes Pigm.*, **14**, 89 (1990).
 25. A. T. Peters, *J. Soc. Dyers Colour.*, **101**, 361 (1985).
 26. J. Griffiths, "Colour and Constitution of Organic Molecules", p.172, Academic Press, London, 1976.
 27. E. Sawicki, *J. Org. Chem.*, **22**, 365 (1957).
 28. J. Griffiths, J. Hill, and B. Fishwick, *Dyes Pigm.*, **15**, 307 (1991).
 29. K. A. Bello and J. Griffiths, *Dyes Pigm.*, **11**, 65 (1989).
 30. J. Griffiths, *J. Soc. Dyers Colour.*, **88**, 106 (1972).